Journal of Sound and Vibration (2000) **233**(5), 835–856
doi:10.1006/jsvi.1999.2852, available online at http://www.idealibrary.com on IDEAL®

MULTIVARIABLE HYBRID MODELS FOR ROTOR-BEARING SYSTEMS

M. ALEYAASIN, M. EBRAHIMI AND R.WHALLEY

Department of Mechanical and Medical Engineering University of Bradford, W. Yorkshire, BD 71DP, England

(*Received* 19 *August* 1999, *and in final form* 29 *November* 1999)

In this paper the flexural vibration of rotors, mounted on fluid film bearings, is considered. The rotor is described by a series of distributed and lumped elements. Frequency-dependent, transfer matrix methods are used to determine the characteristic determinant of the system. Direct search optimization techniques are employed enabling the whirl frequency and system stability to be determined and compared with results obtained from lumped modelling. Thereafter the dynamic stiffness matrix for the system is defined, from which the multivariable frequency response matrix for system can be established. Frequency domain identification techniques are employed enabling the multi-input, multi-output transfer function matrix of the system, to be determined. It is shown that by this method an accurate low order model can be achieved, for feedback control analysis and design.

1. INTRODUCTION

The analysis of the flexural vibrations of rotors, mounted on fluid film bearings, is a principal topic in dynamic studies and in the design of high-speed rotors. Usually, finite element methods are used for the computation of the whirl frequency [1]. However, the high number of natural frequencies obtained by this method have produced large-scale models for multi-mass rotor systems. Furthermore, for the active vibrational control of rotors, the use of a reduced order models are often employed for controller design purposes [2]. Further difficulties arise only when a single actuator is available for control purposes if more than one sensor is used. The reason for this, is the multivariable nature of the rotor-bearing system [3], where the interaction effects must also be considered. Therefore, the use of the transfer function matrix description of the system is a necessary prelude to vibration control studies, where the state-space models in these cases have high number of state variables [2].

The transfer matrix method (TMM) for this process was introduced by Myklestad [4] and later extended by Prohl [5]. The technique was then modified by Lund [6] where distributed shafts connecting lumped discs on bearing supports, are considered to have flexural stiffness, but no mass. This was followed by a combination of transfer matrix and finite element methods [7]. Further modifications which include the effects of distributed shafts, can be found in the literature; see, for example, reference [8], where the elements of the transfer matrix of the distributed elements are frequency dependent.

The stiffness matrix method is well known for the analysis of linearly elastic structures, the members of which are modelled by an equivalent lumped system, see for example reference [9]. This method enables the overall stiffness matrix to be obtained from the individual equations.

0022-460X/00/250835 + 22 $35.00/0

A method used in structural mechanics where the elements of the system are treated as distributed and uniform, by using the frequency-dependent dynamic stiffnesses [10], is known as the dynamic stiffness matrix method (DSMM). These methods are similar owing to the matrix assembling procedure. More recently, this procedure has been referred to as the high-precision finite element method [11].

The dynamic stiffness matrix method is also employed for the vibrational analysis of rotor-bearing systems [12, 13] as an alternative method to the finite element approach and the transfer matrix method. Recently, the theory of distributed-lumped modelling [14] has been employed to establish that TMM and DSMM are equivalent. When implemented for rotors mounted on fluid film bearings, two identical characteristic determinants results. However, the numerical computation of the damped natural frequencies using DSMM yields a significant unavoidable error [15]. Regardless of this limitation, the dynamic stiffness matrix method is described as an accurate technique for frequency response determination [15].

In this paper, the flexural vibration of a rotor-bearing system is analyzed by a combination of TMM and DSMM, In the first step the transfer matrix method is used and the eigenvalues of the system are computed by the Nedler and Mead Simplex search, optimization technique. The whirl frequencies computed thereafter are compared with those obtained from a lumped model of the system.

The computation of the multivariable frequency response matrix of the system by the dynamic stiffness matrix method is also included. This is followed by frequency domain identification from which the multi-input, multi-output transfer function matrix of the system, can be computed. In the case under consideration, two output sensors and two input actuators, and three sensors with two actuators, are investigated. The associated square and non-square, transfer function matrix descriptions of the system are computed for these representations.

2. STABILITY AND WHIRL FREQUENCY, USING TRANSFER MATRIX METHOD

In Figure 1, a rotating shaft representation, consisting of a series of distributed and lumped elements is shown. The number of lumped elements is n and there are $(n + 1)$ distributed elements.

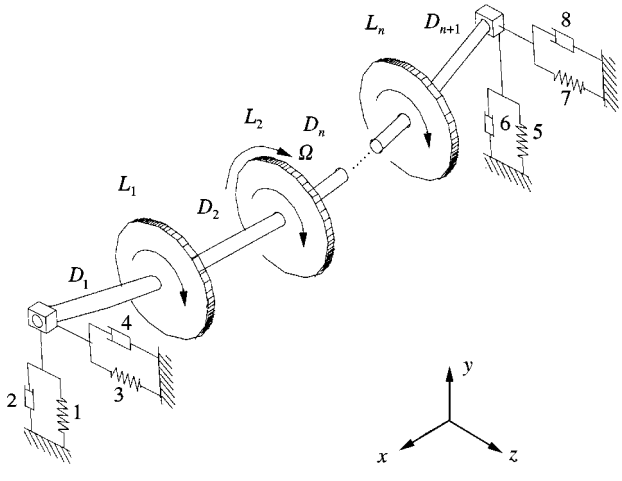

Figure 1. Distributed—Lumped rotor on fluid film bearings: 1—k_{y1y1}; 2—c_{y1y1}; 3—k_{z1z1}; 4—c_{z1z1}; 5—k_{y2y2}; 6—c_{y2y2}; 7—k_{z2z2}; 8—c_{z2z2}.

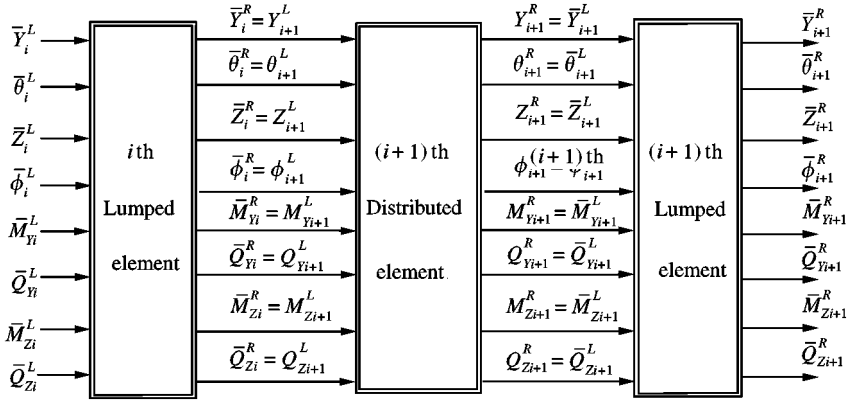

Figure 2. Distributed–lumped parameter model.

The distributed-lumped parameter model for the system is shown in Figure 2. For the distributed part there are left and right-hand terminations each having eight parameters. These are displacement Y_i^L, Y_i^R and Z_i^L, Z_i^R, slopes θ_i^L, θ_i^R and ϕ_i^L, ϕ_i^R, bending moments $M_{y_i}^L$, $M_{y_i}^R$ and $M_{z_i}^L$, $M_{z_i}^R$, shear forces $Q_{y_i}^L$, $Q_{y_i}^R$ and $Q_{z_i}^L$, $Q_{z_i}^R$, for the left and right boundary terminations respectively. For the lumped part there are also left- and right-hand terminations each specified by the above eight parameters. The input to the lumped elements is the output from the distributed elements. The procedures for the derivation of an Euler beam model are exercised for the distributed part while the equations for rigid-body motion are considered for the lumped model [16].

The following relationships exist for the input and output of each distributed, and lumped element, the detailed analysis of which are given in reference [16]. The governing distributed element equation is

$$\begin{bmatrix} Y_i^R \\ \theta_i^R \\ Z_i^R \\ \phi_i^R \\ M_{y_i}^R \\ Q_{y_i}^R \\ M_{z_i}^R \\ Q_{z_i}^R \end{bmatrix} = [\mathbf{\Phi}_d^{(i)}] \begin{bmatrix} Y_i^L \\ \theta_i^L \\ Z_i^L \\ \phi_i^L \\ M_{y_i}^L \\ Q_{y_i}^L \\ M_{z_i}^L \\ Q_{z_i}^L \end{bmatrix}, \tag{1}$$

where $[\mathbf{\Phi}_d^{(i)}]$ is the 8×8 matrix:

$$[\mathbf{\Phi}_d^{(i)}] = \begin{bmatrix} [\mathbf{T}_{ll}^i] & [\mathbf{T}_{lr}^i] \\ [\mathbf{T}_{rl}^i] & [\mathbf{T}_{rr}^i] \end{bmatrix}, \tag{2}$$

where

$$[\mathbf{T}^i_{ll}] = \begin{bmatrix} \dfrac{(\cosh\sqrt{\Gamma}L + \cos\sqrt{\Gamma}L)}{2} & \dfrac{(\sinh\sqrt{\Gamma}L + \sin\sqrt{\Gamma}L)}{2\sqrt{\Gamma}} \\ \dfrac{\sqrt{\Gamma}}{2}(\sinh\sqrt{\Gamma}L - \sin\sqrt{\Gamma}L) & \dfrac{(\cosh\sqrt{\Gamma}L + \cos\sqrt{\Gamma}L)}{2} \\ 0 & 0 \\ 0 & 0 \end{bmatrix}$$

$$\begin{bmatrix} 0 & 0 \\ 0 & 0 \\ \dfrac{(\cosh\sqrt{\Gamma}L + \cos\sqrt{\Gamma}L)}{2} & \dfrac{(\sinh\sqrt{\Gamma}L + \sin\sqrt{\Gamma}L)}{2} \\ \dfrac{\sqrt{\Gamma}}{2}(\sinh\sqrt{\Gamma}L - \sin\sqrt{\Gamma}L) & \dfrac{(\cosh\sqrt{\Gamma}L + \cos\sqrt{\Gamma}L)}{2} \end{bmatrix} \tag{3a}$$

$$[\mathbf{T}^i_{lr}] = \begin{bmatrix} \dfrac{C_0}{2\Gamma}(\cos\sqrt{\Gamma}L - \cosh\sqrt{\Gamma}L) & \dfrac{C_0}{2\Gamma\sqrt{\Gamma}}(\sin\sqrt{\Gamma}L - \sinh\sqrt{\Gamma}L) \\ \dfrac{-C_0}{2\sqrt{\Gamma}}(\sinh\sqrt{\Gamma}L + \sin\sqrt{\Gamma}L) & \dfrac{C_0}{2\Gamma}(\cos\sqrt{\Gamma}L - \cosh\sqrt{\Gamma}L) \\ 0 & 0 \\ 0 & 0 \end{bmatrix}$$

$$\begin{bmatrix} 0 & 0 \\ 0 & 0 \\ \dfrac{C_0}{2\Gamma}(\cos\sqrt{\Gamma}L - \cosh\sqrt{\Gamma}L) & \dfrac{C_0}{2\Gamma\sqrt{\Gamma}}(\sin\sqrt{\Gamma}L + \sinh\sqrt{\Gamma}L) \\ \dfrac{-C_0}{2\sqrt{\Gamma}}(\sinh\sqrt{\Gamma}L + \sin\sqrt{\Gamma}L) & \dfrac{C_0}{2\Gamma}(\cos\sqrt{\Gamma}L - \cosh\sqrt{\Gamma}L) \end{bmatrix} \tag{3b}$$

$$[\mathbf{T}^i_{rl}] = \begin{bmatrix} \frac{\Gamma}{2C_0}(\cos\sqrt{\Gamma}L - \cosh\sqrt{\Gamma}L) & \frac{\sqrt{\Gamma}}{2C_0}(\sin\sqrt{\Gamma}L - \sinh\sqrt{\Gamma}L) \\ \frac{-\Gamma\sqrt{\Gamma}}{2C_0}(\sinh\sqrt{\Gamma}L + \sin\sqrt{\Gamma}L) & \frac{\Gamma}{2C_0}(\cos\sqrt{\Gamma}L - \cosh\sqrt{\Gamma}L) \\ 0 & 0 \\ 0 & 0 \end{bmatrix}$$

$$\begin{bmatrix} 0 & 0 \\ 0 & 0 \\ \frac{\Gamma}{2C_0}(\cos\sqrt{\Gamma}L - \cosh\sqrt{\Gamma}L) & \frac{\sqrt{\Gamma}}{2C_0}(\sin\sqrt{\Gamma}L - \sinh\sqrt{\Gamma}L) \\ \frac{-\Gamma\sqrt{\Gamma}}{2C_0}(\sinh\sqrt{\Gamma}L + \sin\sqrt{\Gamma}L) & \frac{\Gamma}{2C_0}(\cos\sqrt{\Gamma}L - \cosh\sqrt{\Gamma}L) \end{bmatrix} \tag{3c}$$

$$[\mathbf{T}^i_{rr}] = \begin{bmatrix} \frac{1}{2}(\cos\sqrt{\Gamma}L - \cosh\sqrt{\Gamma}L) & \frac{1}{2\sqrt{\Gamma}}(\sinh\sqrt{\Gamma}L + \sin\sqrt{\Gamma}L) \\ \frac{\sqrt{\Gamma}}{2}(\sinh\sqrt{\Gamma}L - \sin\sqrt{\Gamma}L) & \frac{1}{2}(\cosh\sqrt{\Gamma}L + \cos\sqrt{\Gamma}L) \\ 0 & 0 \\ 0 & 0 \end{bmatrix}$$

$$\begin{bmatrix} 0 & 0 \\ 0 & 0 \\ \frac{1}{2}(\cos\sqrt{\Gamma}L - \cosh\sqrt{\Gamma}L) & \frac{1}{2\sqrt{\Gamma}}(\sinh\sqrt{\Gamma}L + \sin\sqrt{\Gamma}L) \\ \frac{\sqrt{\Gamma}}{2}(\sinh\sqrt{\Gamma}L - \sin\sqrt{\Gamma}L) & \frac{1}{2}(\cosh\sqrt{\Gamma}L + \cos\sqrt{\Gamma}L) \end{bmatrix}. \tag{3d}$$

For the lumped parts, the gyroscopic moments and rotary inertia of the discs are included which couples the motions in y and z directions:

$$\begin{bmatrix} \bar{Y}_i^R \\ \bar{\theta}_i^R \\ \bar{Z}_i^R \\ \bar{\phi}_i^R \\ \bar{M}_{y_i}^R \\ \bar{Q}_{y_i}^R \\ \bar{M}_{z_i}^R \\ \bar{Q}_{z_i}^R \end{bmatrix} = [\mathbf{\Phi}_l^{(i)}] \begin{bmatrix} \bar{Y}_i^L \\ \bar{\theta}_i^L \\ \bar{Z}_i^L \\ \bar{\phi}_i^L \\ \bar{M}_{y_i}^L \\ \bar{Q}_{y_i}^L \\ \bar{M}_{z_i}^L \\ \bar{Q}_{z_i}^L \end{bmatrix}, \tag{4}$$

where the $[\mathbf{\Phi}_l^{(i)}]$ in equation (4) is [6]

$$[\mathbf{\Phi}_l^{(i)}] = \begin{bmatrix} \mathbf{D}_{ll}^i & \mathbf{D}_{lr}^i \\ \mathbf{D}_{rl}^i & \mathbf{D}_{rr}^i \end{bmatrix}. \tag{5}$$

and

$$\mathbf{D}_{ll}^i = \begin{bmatrix} 1 & 0 & 0 & 0 \\ 0 & 1 & 0 & 0 \\ 0 & 0 & 1 & 0 \\ 0 & 0 & 0 & 1 \end{bmatrix} = \mathbf{D}_{rr}^i \quad \mathbf{D}_{lr}^i = \begin{bmatrix} 0 & 0 & 0 & 0 \\ 0 & 0 & 0 & 0 \\ 0 & 0 & 0 & 0 \\ 0 & 0 & 0 & 0 \end{bmatrix} \tag{6a}$$

$$\mathbf{D}_{rl}^i = \begin{bmatrix} 0 & J_t s^2 & 0 & \Omega J_p s \\ ms^2 & 0 & 0 & 0 \\ 0 & -\Omega J_p s & 0 & J_t s^2 \\ 0 & 0 & ms^2 & 0 \end{bmatrix} \tag{6b}$$

where in equation (6b) J_p and J_t are the polar and transverse moments of inertia of lumped disc and Γ in equation (3) is

$$\Gamma = s\sqrt{L_0 C_0} \tag{7}$$

and in equation (7)

$$L_0 = \rho A, \tag{8}$$

$$C_0 = \frac{1}{EI}. \tag{9}$$

In equations (1)–(9), s is the Laplace variable, m is the mass of each lumped element, Ω is the rotational speed of the shaft, ρ is the density of the shaft material, A is the cross-sectional area, E is the modulus of elasticity and I is the moment of inertia of the cross-section in bending, for each distributed element. The polar moment of inertia of the lumped disc is J_p and L is the length of each distributed element.

The transfer matrix for the fluid film bearings could be expressed by the stiffness and damping of the fluid film, as indicated in Figure 1, yielding the form

$$\begin{bmatrix} \hat{Y}_i^R \\ \hat{\theta}_i^R \\ \hat{Z}_i^R \\ \hat{\phi}_i^R \\ \hat{M}_{y_i}^R \\ \hat{Q}_{y_i}^R \\ \hat{M}_{z_i}^R \\ \hat{Q}_{z_i}^R \end{bmatrix} = [\mathbf{\Phi}_b^{(i)}] \begin{bmatrix} \hat{Y}_i^L \\ \hat{\theta}_i^L \\ \hat{Z}_i^L \\ \hat{\phi}_i^L \\ \hat{M}_{y_i}^L \\ \hat{Q}_{y_i}^L \\ \hat{M}_{z_i}^L \\ \hat{Q}_{z_i}^L \end{bmatrix}, \tag{10}$$

where the $[\mathbf{\Phi}_b^{(i)}]$ in equation (10) is [6]

$$[\mathbf{\Phi}_b^{(i)}] = \begin{bmatrix} \mathbf{B}_{ll}^i & \mathbf{B}_{lr}^i \\ \mathbf{B}_{rl}^i & \mathbf{B}_{rr}^i \end{bmatrix}, \tag{11}$$

$$\mathbf{B}_{ll}^i = \mathbf{B}_{rr}^i = \begin{bmatrix} 1 & 0 & 0 & 0 \\ 0 & 1 & 0 & 0 \\ 0 & 0 & 1 & 0 \\ 0 & 0 & 0 & 1 \end{bmatrix}, \quad \mathbf{B}_{lr}^i = \begin{bmatrix} 0 & 0 & 0 & 0 \\ 0 & 0 & 0 & 0 \\ 0 & 0 & 0 & 0 \\ 0 & 0 & 0 & 0 \end{bmatrix}, \tag{12a}$$

$$\mathbf{B}_{rl}^i = \begin{bmatrix} 0 & 0 & 0 & 0 \\ (K_{yy} + sC_{yy}) & 0 & (K_{yz} + sC_{yz}) & 0 \\ 0 & 0 & 0 & 0 \\ (K_{zy} + sC_{zy}) & 0 & (K_{zz} + sC_{zz}) & 0 \end{bmatrix}, \tag{12b}$$

and K_{yy}, K_{yz}, K_{zz}, K_{zy} are the stiffness of the bearings and C_{yy}, C_{yz}, C_{zz}, C_{zy} are the damping coefficients where the indices yz and zy indicate cross-coupled values.

According to Figures 1 and 2, $\hat{Y}_1^L$, $\hat{\theta}_1^L$, $\hat{Z}_1^L$, $\hat{M}_{y1}^L$, $\hat{Q}_{y1}^L$, $\hat{M}_{z1}^L$, $\hat{Q}_{z1}^L$ are the values for the left end of the first bearing and $\hat{Y}_2^R$, $\hat{\theta}_2^R$, $\hat{Z}_2^R$, $\hat{M}_{y2}^R$, $\hat{Q}_{y2}^R$, $\hat{M}_{z2}^R$, $\hat{Q}_{z2}^R$ are the values for the right end of the second bearing. If the transfer matrix of the ith distributed element D_i is $[\mathbf{\Phi}_d^{(i)}]$ and the transfer matrix of the ith lumped element L_i is $[\mathbf{\Phi}_l^{(i)}]$, then the transfer matrix of the overall system $[\mathbf{T}]$ relating the above-mentioned values for the left and right ends can be computed as

$$\begin{bmatrix} \hat{Y}_2^R \\ \hat{\theta}_2^R \\ \hat{Z}_2^R \\ \hat{\phi}_2^R \\ \hat{M}_{y_2}^R \\ \hat{Q}_{y_2}^R \\ \hat{M}_{z_2}^R \\ \hat{Q}_{z_2}^R \end{bmatrix} = [\mathbf{T}] \begin{bmatrix} \hat{Y}_1^L \\ \hat{\theta}_1^L \\ \hat{Z}_1^L \\ \hat{\phi}_1^L \\ \hat{M}_{y_1}^L \\ \hat{Q}_{y_1}^L \\ \hat{M}_{z_1}^L \\ \hat{Q}_{z_1}^L \end{bmatrix}, \tag{13}$$

where $[\mathbf{T}]$ in equation (13) is

$$[\mathbf{T}] = [\mathbf{\Phi}_b^{(2)}][\mathbf{\Phi}_d^{(n+1)}]\left(\prod_{t=0}^{n-1}([\mathbf{\Phi}_l^{(n-1)}][\mathbf{\Phi}_d^{(n-1)}])\right)[\mathbf{\Phi}_b^{(1)}]. \tag{14}$$

Finally, equation (13) can be expanded using the elements of the $[\mathbf{T}]$ matrix yielding

$$\hat{Y}_2^R = T_{11}\hat{Y}_1^L + T_{12}\hat{\theta}_1^L + T_{13}\hat{Z}_1^L + T_{14}\hat{\phi}_1^L + T_{15}\hat{M}_{y_1}^L + T_{16}\hat{Q}_{y_1}^L + T_{17}\hat{M}_{z_1}^L + T_{18}\hat{Q}_{z_1}^L, \tag{15}$$

$$\hat{\theta}_2^R = T_{21}\hat{Y}_1^L + T_{22}\hat{\theta}_1^L + T_{23}\hat{Z}_1^L + T_{24}\hat{\phi}_1^L + T_{25}\hat{M}_{y_1}^L + T_{26}\hat{Q}_{y_1}^L + T_{27}\hat{M}_{z_1}^L + T_{28}\hat{Q}_{z_1}^L, \tag{16}$$

$$\hat{Z}_2^R = T_{31}\hat{Y}_1^L + T_{32}\hat{\theta}_1^L + T_{33}\hat{Z}_1^L + T_{34}\hat{\phi}_1^L + T_{35}\hat{M}_{y_1}^L + T_{36}\hat{Q}_{y_1}^L + T_{37}\hat{M}_{z_1}^L + T_{38}\hat{Q}_{z_1}^L, \tag{17}$$

$$\hat{\phi}_2^R = T_{41}\hat{Y}_1^L + T_{42}\hat{\theta}_1^L + T_{43}\hat{Z}_1^L + T_{44}\hat{\phi}_1^L + T_{45}\hat{M}_{y_1}^L + T_{46}\hat{Q}_{y_1}^L + T_{47}\hat{M}_{z_1}^L + T_{48}\hat{Q}_{z_1}^L, \tag{18}$$

$$\hat{M}_{y_2}^R = T_{51}\hat{Y}_1^L + T_{52}\hat{\theta}_1^L + T_{53}\hat{Z}_1^L + T_{54}\hat{\phi}_1^L + T_{55}\hat{M}_{y_1}^L + T_{56}\hat{Q}_{y_1}^L + T_{57}\hat{M}_{z_1}^L + T_{58}\hat{Q}_{z_1}^L, \tag{19}$$

$$\hat{Q}_{y_2}^R = T_{61}\hat{Y}_1^L + T_{62}\hat{\theta}_1^L + T_{63}\hat{Z}_1^L + T_{64}\hat{\phi}_1^L + T_{65}\hat{M}_{y_1}^L + T_{66}\hat{Q}_{y_1}^L + T_{67}\hat{M}_{z_1}^L + T_{68}\hat{Q}_{z_1}^L, \tag{20}$$

$$\hat{M}_{z_2}^R = T_{71}\hat{Y}_1^L + T_{72}\hat{\theta}_1^L + T_{73}\hat{Z}_1^L + T_{74}\hat{\phi}_1^L + T_{75}\hat{M}_{y_1}^L + T_{76}\hat{Q}_{y_1}^L + T_{77}\hat{M}_{z_1}^L + T_{78}\hat{Q}_{z_1}^L, \tag{21}$$

$$\hat{Q}_{z_2}^R = T_{81}\hat{Y}_1^L + T_{82}\hat{\theta}_1^L + T_{83}\hat{Z}_1^L + T_{84}\hat{\phi}_1^L + T_{85}\hat{M}_{y_1}^L + T_{86}\hat{Q}_{y_1}^L + T_{87}\hat{M}_{z_1}^L + T_{88}\hat{Q}_{z_1}^L. \tag{22}$$

For the configuration in Figure 1 the values of $\hat{M}_{y_1}^L = 0$, $\hat{Q}_{y_1}^L = 0$, $\hat{M}_{y_1}^L = 0$, $\hat{Q}_{z_1}^L = 0$ are for the left-hand end of the first bearing and the values of $\hat{M}_{z_2}^R = 0$, $\hat{Q}_{y_2}^R = 0$, $\hat{M}_{y_2}^R = 0$, $\hat{Q}_{z_2}^R = 0$ are for the right-hand end of the second bearing. Therefore, equations (19)–(22) are simply

$$T_{51}\hat{Y}_1^L + T_{52}\hat{\theta}_1^L + T_{53}\hat{Z}_1^L + T_{54}\hat{\phi}_1^L = 0, \tag{23}$$

$$T_{61}\hat{Y}_1^L + T_{62}\hat{\theta}_1^L + T_{63}\hat{Z}_1^L + T_{64}\hat{\phi}_1^L = 0, \tag{24}$$

$$T_{71}\hat{Y}_1^L + T_{72}\hat{\theta}_1^L + T_{73}\hat{Z}_1^L + T_{74}\hat{\phi}_1^L = 0, \tag{25}$$

$$T_{81}\hat{Y}_1^L + T_{82}\hat{\theta}_1^L + T_{83}\hat{Z}_1^L + T_{84}\hat{\phi}_1^L = 0. \tag{26}$$

In order to obtain a non-trivial solution for equations (23)–(26) the following determinant must be zero:

$$R = \begin{bmatrix} T_{51} & T_{52} & T_{53} & T_{54} \\ T_{61} & T_{62} & T_{63} & T_{64} \\ T_{71} & T_{72} & T_{73} & T_{74} \\ T_{81} & T_{82} & T_{83} & T_{84} \end{bmatrix} = 0. \tag{27}$$

The damped natural frequency of the system could be computed by determining the roots of this irrational characteristic equation (27). This procedure will be shown via a worked example in the next section.

3. FREQUENCY RESPONSE COMPUTATION BY THE DYNAMIC STIFFNESS MATRIX METHOD

In the formulation of the dynamic stiffness matrix method, the force and displacement vectors must be defined as

$$\mathbf{q}_i^R = \begin{bmatrix} Y_i^R \\ \theta_i^R \\ Z_i^R \\ \phi_i^R \end{bmatrix}, \quad \mathbf{q}_i^L = \begin{bmatrix} Y_i^L \\ \theta_i^L \\ Z_i^L \\ \phi_i^L \end{bmatrix}, \tag{28}$$

$$\mathbf{Q}_i^L = \begin{bmatrix} M_{y_i}^L \\ Q_{y_i}^L \\ M_{z_i}^L \\ Q_{z_i}^L \end{bmatrix}, \quad \mathbf{Q}_i^R = \begin{bmatrix} M_{y_i}^R \\ Q_{y_i}^R \\ M_{z_i}^R \\ Q_{z_i}^R \end{bmatrix}. \tag{29}$$

Then equations (1) and (2) could also be expressed in the following form:

$$\begin{bmatrix} \mathbf{q}_i^R \\ \mathbf{Q}_i^R \end{bmatrix} = \begin{bmatrix} [\mathbf{T}_{ll}^i] & [\mathbf{T}_{lr}^i] \\ [\mathbf{T}_{rl}^i] & [\mathbf{T}_{rr}^i] \end{bmatrix} \begin{bmatrix} \mathbf{q}_i^L \\ \mathbf{Q}_i^L \end{bmatrix}. \tag{30}$$

Equation (30) could be converted into a dynamic stiffness form in which all the elements of the matrix are stiffness coefficients. This conversion is possible for distributed shaft elements since

$$\begin{bmatrix} \mathbf{Q}_i^L \\ \mathbf{Q}_i^R \end{bmatrix} = \begin{bmatrix} [\mathbf{K}_{ll}^i] & [\mathbf{K}_{lr}^i] \\ [\mathbf{K}_{rl}^i] & [\mathbf{K}_{rr}^i] \end{bmatrix} \begin{bmatrix} \mathbf{q}_i^L \\ \mathbf{q}_i^R \end{bmatrix}. \tag{31}$$

The elements of the dynamic stiffness matrix in equation (31) could be expressed in terms of transfer matrix elements detailed in reference [16] as

$$[\mathbf{K}_{ll}^i] = -[\mathbf{T}_{lr}^i]^{-1}[\mathbf{T}_{ll}^i] \qquad [\mathbf{K}_{lr}^i] = [\mathbf{T}_{lr}^i]^{-1} \qquad [\mathbf{K}_{rr}^i] = [\mathbf{T}_{rr}^i][\mathbf{T}_{lr}^i]^{-1} \tag{32}$$

$$[\mathbf{K}_{rl}^i] = [\mathbf{T}_{rl}^i] - [\mathbf{T}_{rr}^i][\mathbf{T}_{rl}^i]^{-1}[\mathbf{T}_{ll}^i] \tag{33}$$

Generally, when a part of the rotor bearing system, consists of n successive distributed shaft elements, then the overall dynamic stiffness matrix could be expressed as [15]

$$\begin{bmatrix} [\mathbf{Q}_l^L] \\ \mathbf{0} \\ \mathbf{0} \\ \mathbf{0} \\ \mathbf{0} \\ \vdots \\ [\mathbf{Q}_{ll}^L] \end{bmatrix} = \begin{bmatrix} [\mathbf{K}_{ll}^1] & [\mathbf{K}_{lr}^1] & \mathbf{0} & \mathbf{0} & \mathbf{0} & \cdots & \mathbf{0} \\ [\mathbf{K}_{rl}^1] & [\mathbf{K}_{rr}^1 - \mathbf{K}_{ll}^2] & -[\mathbf{K}_{lr}^2] & \mathbf{0} & \mathbf{0} & \cdots & \mathbf{0} \\ \mathbf{0} & [\mathbf{K}_{rl}^2] & [\mathbf{K}_{rr}^2 - \mathbf{K}_{ll}^3] & -[\mathbf{K}_{lr}^3] & \mathbf{0} & \cdots & \mathbf{0} \\ \mathbf{0} & \mathbf{0} & \ddots & \ddots & \ddots & \mathbf{0}\cdots & \mathbf{0} \\ \mathbf{0} & \mathbf{0} & \mathbf{0}\cdots & [\mathbf{K}_{rl}^{i-1}] & [\mathbf{K}_{rr}^{i-1} - \mathbf{K}_{ll}^i] & -[\mathbf{K}_{lr}^i] & \cdots\mathbf{0} \\ \mathbf{0} & \mathbf{0} & \cdots & \mathbf{0} & \ddots & \ddots & \ddots\mathbf{0} \\ \mathbf{0} & \mathbf{0} & \mathbf{0} & \cdots & \mathbf{0} & [\mathbf{K}_{rl}^{n-1}] & [\mathbf{K}_{rr}^{n-1}] \end{bmatrix} \begin{bmatrix} [\mathbf{q}_1^L] \\ [\mathbf{q}_2^L] \\ [\mathbf{q}_3^L] \\ \vdots \\ [\mathbf{q}_i^L] \\ \vdots \\ [\mathbf{q}_n^L] \end{bmatrix}. \tag{34}$$

From equations (5) and (6) for the ith disc lumped elements the dynamic stiffness matrix form could not be expressed in the form of equation (31). However, an alternative form could be written as [17]

$$\mathbf{Q}_{i+1}^{L} - \mathbf{Q}_{i}^{R} = \mathbf{D}_{rl}^{i}\mathbf{q}_{i+1}^{L}. \tag{35}$$

Similarly from equations (11) and (12), for first lumped bearing,

$$-\hat{\mathbf{Q}}_{1}^{L} + \mathbf{Q}_{1}^{L} = \mathbf{B}_{rl}^{l}\mathbf{q}_{1}^{L} \tag{36}$$

and for the second lumped bearing,

$$\hat{\mathbf{Q}}_{2}^{R} - \mathbf{Q}_{n}^{R} = \mathbf{B}_{rl}^{2}\mathbf{q}_{n}^{R}. \tag{37}$$

According to Figure 1, when the rotor-bearing system consists of n distributed shaft elements connected by n lumped discs and is supported on two bearings at the left and right ends, uising equations (35)–(37) and (33), the equations for the flexural vibrations of the rotor could be expressed by a dynamic stiffness matrix form as follows:

$$\begin{bmatrix} [\hat{\mathbf{Q}}_1^L] \\ \mathbf{0} \\ \mathbf{0} \\ \mathbf{0} \\ \mathbf{0} \\ \vdots \\ [\hat{\mathbf{Q}}_2^R] \end{bmatrix} = \begin{bmatrix} [\mathbf{K}_{ll}^1 + \mathbf{B}_{rl}^1] & [\mathbf{K}_{lr}^1] & \mathbf{0} & \mathbf{0} \\ [\mathbf{K}_{rl}^1] & [\mathbf{K}_{rr}^1 - \mathbf{K}_{ll}^2 + \mathbf{D}_{rl}^1] & -[\mathbf{K}_{lr}^2] & \mathbf{0} \\ \mathbf{0} & [\mathbf{K}_{rl}^2] & [\mathbf{K}_{rr}^2 - \mathbf{K}_{ll}^3 + \mathbf{D}_{rl}^2] & -[\mathbf{K}_{lr}^3] \\ \mathbf{0} & \mathbf{0} & \ddots & \ddots \\ \mathbf{0} & \mathbf{0} & \mathbf{0}\cdots & [\mathbf{K}_{rl}^{i-1}] \\ \mathbf{0} & \mathbf{0} & \cdots & \mathbf{0} \\ \mathbf{0} & \mathbf{0} & \mathbf{0} & \cdots \end{bmatrix}$$

$$\begin{bmatrix} \mathbf{0} & \cdots & \mathbf{0} \\ \mathbf{0} & \cdots & \mathbf{0} \\ \mathbf{0} & \cdots & \mathbf{0} \\ \ddots & \mathbf{0}\cdots & \mathbf{0} \\ [\mathbf{K}_{rr}^{i-1} - \mathbf{K}_{ll}^{i} + \mathbf{D}_{rl}^{i-1}] & -[\mathbf{K}_{lr}^{i}] & \cdots\mathbf{0} \\ \ddots & \ddots & \ddots\mathbf{0} \\ \mathbf{0} & [\mathbf{K}_{rl}^{m-1}] & [\mathbf{K}_{rr}^{m-1} + \mathrm{B}_{rl}^{m}] \end{bmatrix} \begin{bmatrix} [\mathbf{q}_1^L] \\ [\mathbf{q}_2^L] \\ [\mathbf{q}_3^L] \\ \vdots \\ [\mathbf{q}_1^L] \\ \vdots \\ [\mathbf{q}_n^R] \end{bmatrix}. \tag{38}$$

where equation (38) is the generalized form of the system equations in reference [14]. For the purpose of frequency response determination, consider the external forces applied to the ith lumped element, designated by $[\bar{\mathbf{Q}}_i]$ and the resulting displacement designated by $[\bar{\mathbf{q}}_i]$. Then the equations of motion could be expressed in terms of the flexibility matrix as

$$\begin{bmatrix} [\bar{\mathbf{q}}_1] \\ [\bar{\mathbf{q}}_2] \\ [\bar{\mathbf{q}}_3] \\ \vdots \\ [\bar{\mathbf{q}}_i] \\ \vdots \\ [\bar{\mathbf{q}}_n] \end{bmatrix} = \mathbf{\Lambda} \begin{bmatrix} [\bar{\mathbf{Q}}_1] \\ [\bar{\mathbf{Q}}_2] \\ [\bar{\mathbf{Q}}_3] \\ \vdots \\ [\bar{\mathbf{Q}}_i] \\ \vdots \\ [\bar{\mathbf{Q}}_n] \end{bmatrix}. \tag{39}$$

The flexibility matrix in equation (39) is

$$\mathbf{\Lambda} = \begin{bmatrix} [\mathbf{K}_{ll}^1 + \mathbf{B}_{rl}^1] & [\mathbf{K}_{lr}^1] & \mathbf{0} & \mathbf{0} \\ [\mathbf{K}_{rl}^1] & [\mathbf{K}_{rr}^1 - \mathbf{K}_{ll}^2 + \mathbf{D}_{rl}^1] & -[\mathbf{K}_{lr}^2] & \mathbf{0} \\ \mathbf{0} & [\mathbf{K}_{rl}^2] & [\mathbf{K}_{rr}^2 - \mathbf{K}_{ll}^3 + \mathbf{D}_{rl}^2] & -[\mathbf{K}_{lr}^3] \\ \mathbf{0} & \mathbf{0} & \ddots & \ddots \\ \mathbf{0} & \mathbf{0} & \mathbf{0}\cdots & [\mathbf{K}_{rl}^{i-1}] \\ \vdots & \vdots & \cdots & 0 \\ \mathbf{0} & \mathbf{0} & \mathbf{0} & \cdots \end{bmatrix}$$

$$\begin{bmatrix} \mathbf{0} & \cdots & \mathbf{0} \\ \mathbf{0} & \cdots & \mathbf{0} \\ \mathbf{0} & \cdots & \mathbf{0} \\ \ddots & \mathbf{0}\cdots & \vdots \\ [\mathbf{K}_{rr}^{i-1} - \mathbf{K}_{ll}^{i} + \mathbf{D}_{rl}^{i-1}] & -[\mathbf{K}_{lr}^{i}] & \cdots \mathbf{0} \\ \ddots & \ddots & \ddots \mathbf{0} \\ \mathbf{0} & [\mathbf{K}_{rl}^{n-1}] & [\mathbf{K}_{rr}^{n-1} + \mathbf{B}_{rl}^{n}] \end{bmatrix}^{-1}. \quad (40)$$

For rotors mounted on fluid film bearings, the force vectors at the left of the first bearing and at the right of the second bearing vanishes:

$$[\hat{\mathbf{Q}}_1^L] = \mathbf{0} \quad \text{and} \quad [\hat{\mathbf{Q}}_2^R] = \mathbf{0}. \quad (41)$$

Considering equations (41) the system of equations (38) has non-trivial solution if the following determinant is zero:

$$R = |\mathbf{\Lambda}^{-1}| = 0. \quad (42)$$

Recently, the authors have shown the equivalence of the characteristic determinants in TMM demonstrated in equation (27) with one in the DSMM displayed in equation (42). However, they pointed out that numerical computation considers the denominator terms also in equation (42) and this leads to a significant error in the computation of the damped natural frequencies by the DSMM [15].

Meanwhile the vibration of the mth lumped disc in vertical y direction which results from the vertical excitation force at lth lumped element can be computed easily using the flexibility matrix in equation (40) so that

$$G_{lm}(\mathrm{j}\omega) = \underset{r=4m-3, s=4l-2}{\mathbf{\Lambda}_{rs}(\mathrm{j}\omega)}, \quad (43)$$

where $G_{lm}(\mathrm{j}\omega)$ in equation (43) is the frequency response function. Frequency response data can be obtained from each transfer function, so that a vector of frequency response data, as a function of ω could be written as

$$G_{pp}(\mathrm{j}.\omega) = x_{pp} + \mathrm{j}.y_{pp}, \quad (44)$$

$$G_{pq}(\mathrm{j}.\omega) = x_{pq} + \mathrm{j}.y_{pq}. \quad (45)$$

Although there are some techniques for the identification of models from frequency response data, time domain, state-space realizations are often employed [18]. If each set of frequency response data is considered separately, then one can estimate any rational transfer function [19]. Since the results obtained through simulation do not include noise, the authors have investigated the time response from the frequency response data, using the inverse Fourier transform [20]. The results show responses similar to those from a second order system model. This leads to the application of a second order identification algorithm. The second order transfer function estimates, enabling the determination of the transfer function from the frequency response data in equations (44) and (45) result in the following form:

$$G'_{pp}(s) = \frac{1}{(m_{pp}s^2 + c_{pp}s + k_{pp})}, \tag{46}$$

$$G'_{pq}(s) = \frac{1}{(m_{pq}s^2 + c_{pq}s + k_{pq})}. \tag{47}$$

For the mass, damping, and stiffness coefficients to have the same roots as the determinant in equation (27), equations (46) and (47) can be written as

$$G'_{pp}(s) = \frac{1}{m_{pp}(s^2 + 2as + a^2 + b^2)}, \tag{48}$$

$$G'_{pq}(s) = \frac{1}{m_{pq}(s^2 + 2as + a^2 + b^2)}, \tag{49}$$

where $s = -a \pm jb$ are the roots of the determinant.

If $y_{pp}^{(\max)}$ and $y_{pq}^{(\max)}$ are the maximum absolute values of the frequency response function of the actual system, in equations (44) and (45), then the second order systems models described in equations (46) and (47) have the same maximum absolute value, as shown in reference [21]:

$$y_{pp}^{(\max)} = \frac{2m_{pp}}{c_{pp}\sqrt{4k_{pp}m_{pp} - c_{pp}^2}}, \tag{50}$$

$$y_{pq}^{(\max)} = \frac{2m_{pq}}{c_{pq}\sqrt{4k_{pq}m_{pq} - c_{pq}^2}}, \tag{51}$$

By comparing equations (46) and (47) with equations (48) and (49) the following equations can be obtained:

$$c_{pp} = 2am_{pp}, \qquad k_{pp} = m_{pp}(a^2 + b^2) \tag{52, 53}$$

$$c_{pq} = 2am_{pq}, \qquad k_{pq} = m_{pq}(a^2 + b^2) \tag{54, 55}$$

By substituting equations (52)–(55) into equations (50) and (51) the following relationships can be obtained.

$$m_{pp} = \frac{1}{2aby_{pp}^{(\max)}}, \tag{56}$$

$$m_{pq} = \frac{1}{2aby_{pq}^{(\max)}}. \tag{57}$$

The parameters of the second order models have the same maximum absolute value as the frequency response function and also the poles are equal to the roots of the determinant in equation (27). As will be seen in the next section this method of identification leads to the optimal matching of the actual and estimated frequency response data.

4. NUMERICAL EXAMPLE AND APPLICATION

A rotor-bearing system which is shown in Figure 3 consists of three lumped steel discs each with thickness of $t = 50$ mm, diameter of 100 mm connected by four distributed shaft elements each with length of $L = 400$ mm and diameter $D = 25{\cdot}4$ mm. This example is considered by Burrows and Sahinkaya. [3] were lumped modelling and vibration control of rotating machanics are investigated. The rotor with angular velocity of $\Omega = 360$ rad/s is supported by two identical fluid film bearings each with the length $l = 16{\cdot}9$ mm, and the journal radius $R = 25{\cdot}4$ mm. The radial clearance is $c = 0{\cdot}127$ mm and the lubricant viscosity is $\mu = 0{\cdot}015$ s/m^2. Using the above data the stiffness and damping of the bearings could be computed according to the procedure outlined in Appendix A. This enables further computation as following.

1. Compute $I = \pi D^4/64$ and then $C_0 = 1/EI$ and also $L_0 = \rho A = \pi\rho D^2/4$ for the distributed shaft parts.
2. Choose a value for ω and σ, put $s = j\omega + \sigma$ in equation (7) then compute $\sqrt{\Gamma}$ for each distributed part.

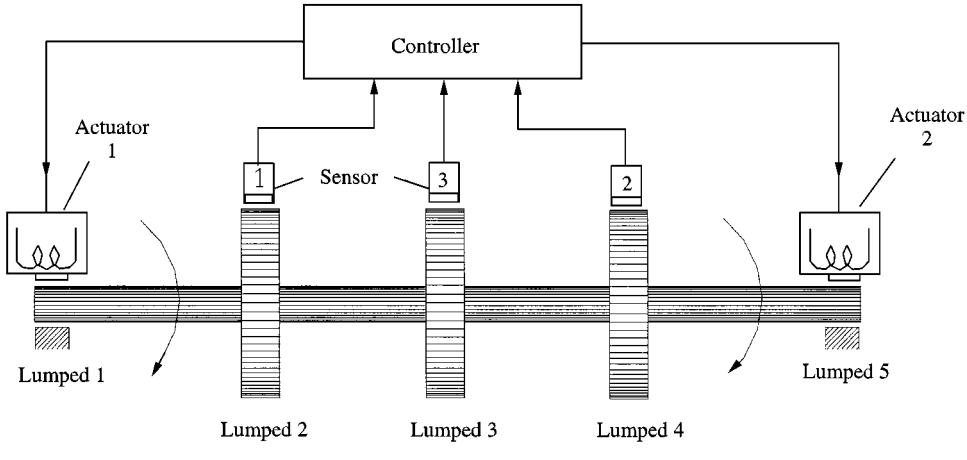

Figure 3. Schematic representation of the rotating shaft system.

3. Using the values of L, Γ, C_0, compute the matrix $[\mathbf{\Phi}_d]$ for each distributed part from equations (2) and (3).
4. Using the values of Ω, s, J_p, J_d, m to compute the matrix $[\mathbf{\Phi}_l]$ for each lumped part from equations (5) and (6).
5. Using the values of l, R, μ, c. Ω and the load carried by the bearing P find the stiffness and damping constants of the bearings from equations (1a) to (10a) and then compute $[\mathbf{\Phi}_b]$ from equations (11) and (12).
6. Find the elements of matrix $\mathbf{T}$ from equation (14) and then compute the value of R from equation (27).
7. Continue steps 2–6 by choosing further values ω and σ thereafter compute R. When R is minimized the damped natural frequency has been determined.

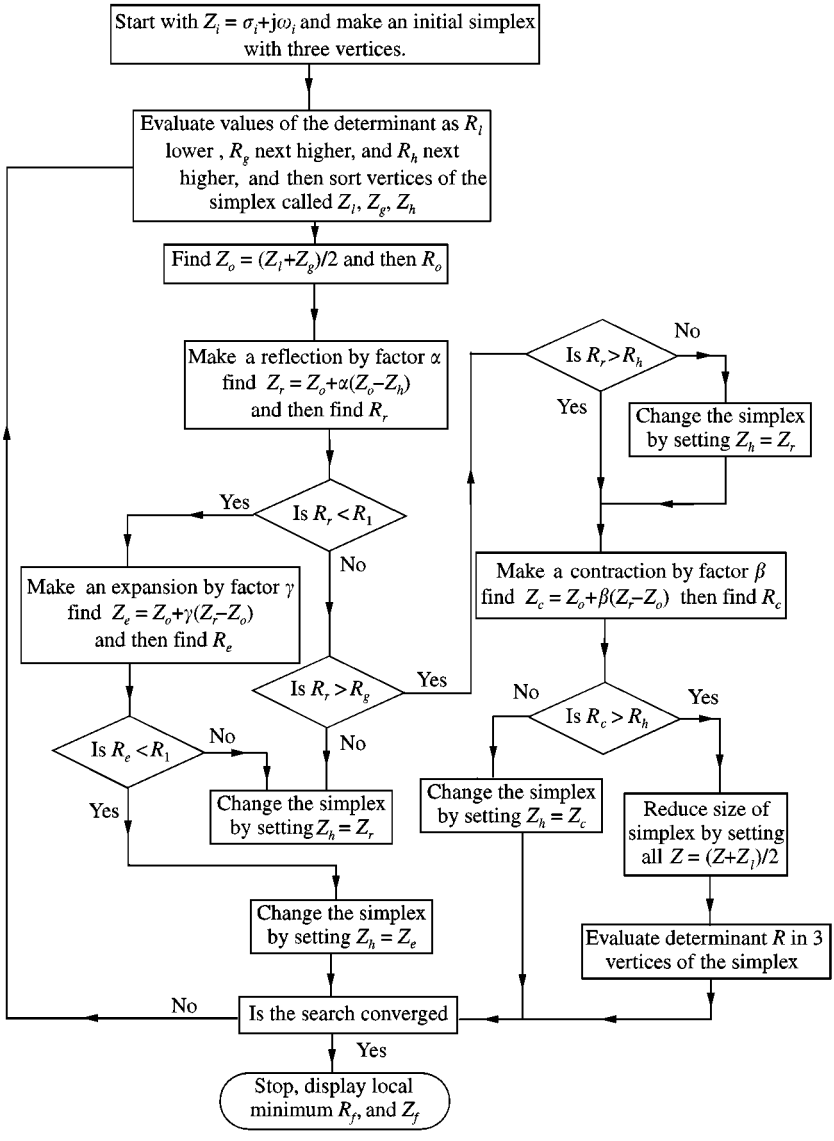

Figure 4. Flow chart for the Nedler and Meads Simplex direct search method.

For minimization of the determinant, the Nedler and Mead simplex search method which is a direct search optimization technique, is used, for minimizing multivariable functions [22].

The algorithm for this technique for searching for the minimum value of the determinant is described by the flow chart in Figure 4. The method accepts the initial values ω_i and σ_i and forms an initial simplex with three vertices. The values of the determinant R_h, R_g and R_l and the vertices Z_h, Z_g and Z_l forms the simplex which is changed in each operation. The search consists of three basic operations known as *reflection*, *expansion* and contraction which are described in Figure 4.

After a convergence test [23], the complex root of the irrational characteristics determinant $Z_f = \sigma_f + j\omega_f$ is found which minimizes R, thereby giving the damped natural frequency of the system model. In Table 1 the damped natural frequency of the system is computed for three different starting values of $Z_i = \sigma_i + j\omega_i$. The results show that this search finally converges to the accurate damped natural frequency of the system, and the number of iterations depends on the starting values.

In Figure 5, the three-dimensional graph shows the value of the determinant R versus the real and imaginary parts of the root, σ and ω respectively. The minimum value of the

TABLE 1

$\sigma_f + j\omega_f$ is computed using the Nedler and Meads simplex optimization method

Initial values ω_i and σ_i for starting optimisation procedure	Final values ω_f and σ_f by using Nedler and Meads simplex method in METLAB	Number of iterations in optimization by Nedler and Meads method	Minimum value of the determination in optimization by Nedler and Meads method
$\omega_i = 10$ rad/s $\sigma_i = -10\ s^{-1}$	$\omega_f = 112{\cdot}11$ rad/s $\sigma_f = -2{\cdot}722\ s^{-1}$	$N = 323$	$R = 3{\cdot}545 \times 10^{19}$
$\omega_i = 100$ rad/s $\sigma_i = -100\ s^{-1}$	$\omega_f = 110{\cdot}60$ rad/s $\sigma_f = -3{\cdot}054\ s^{-1}$	$N = 464$	$R = 3{\cdot}735 \times 10^{19}$
$\omega_i = 200$ rad/s $\sigma_i = -20\ s^{-1}$	$\omega_f = 110{\cdot}60$ rad/s $\sigma_f = -3{\cdot}054\ s^{-1}$	$N = 409$	$R = 3{\cdot}735 \times 10^{19}$

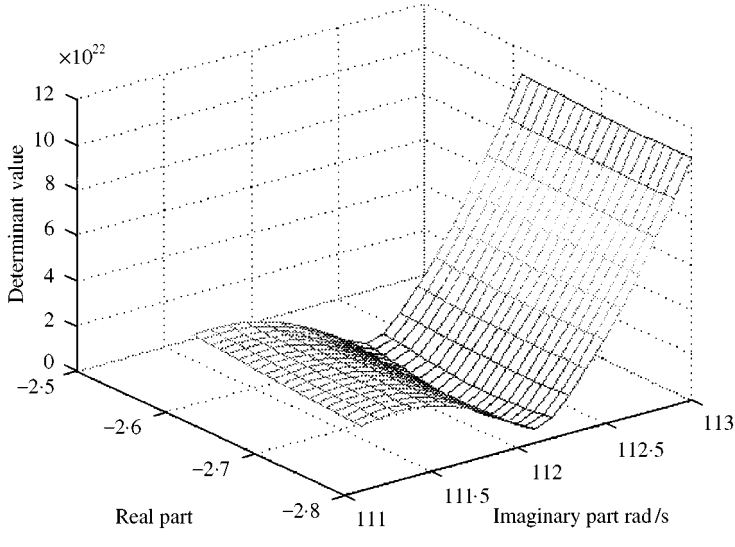

Figure 5. Minimum value of the determinant at whirl frequency is $-2{\cdot}27 \pm 112{\cdot}1$j.

determinant is $R = 3{\cdot}55 \times 10^{19}$ for $s = -2{\cdot}72 + 112{\cdot}1\mathrm{j}$ which determines the damped natural frequency of the system so that $\omega = 112$ rad/s, is the whirl frequency which is often less than half of the rotational frequency as reported in the literature [16]. The result obtained using lumped modelling, excludes the gyroscopic effects of the discs and is 136 rad/s [3]. This accounts for the 13% difference in the two results. The finite element method result strongly depends on the number and degrees of freedom of the elements [1]. The validity of our approach moreover is indicated by the damped natural frequency 112 rad/s being less than half of the rotational frequency of the rotor [6] while the negative real part ensures the stability of the system.

For the system in Figure 3, in the case where three sensors are used to measure the vertical vibration of the lumped discs, while the control force is applied through the bearings, the system of equations for the flexural vibrations in equation (39) could be expressed as

$$\begin{bmatrix} \hat{\mathbf{q}}_1 \\ \bar{\mathbf{q}}_1 \\ \bar{\mathbf{q}}_3 \\ \bar{\mathbf{q}}_2 \\ \hat{\mathbf{q}}_2 \end{bmatrix} = \overset{5}{\mathbf{\Lambda}} \begin{bmatrix} \hat{\mathbf{Q}}_1 \\ \bar{\mathbf{Q}}_1 \\ \bar{\mathbf{Q}}_3 \\ \bar{\mathbf{Q}}_2 \\ \hat{\mathbf{Q}}_2 \end{bmatrix}, \tag{58}$$

where the flexibility matrix of the system would be

$$\overset{5}{\mathbf{\Lambda}} = \begin{bmatrix} [\mathbf{K}_{ll}^1 + \mathbf{B}_{rl}^1] & [\mathbf{K}_{lr}^1] & \mathbf{0} & \mathbf{0} & \mathbf{0} \\ [\mathbf{K}_{rl}^1] & [\mathbf{K}_{rr}^1 - \mathbf{K}_{ll}^2 + \mathbf{D}_{rl}^1] & -[\mathbf{K}_{lr}^2] & \mathbf{0} & \mathbf{0} \\ \mathbf{0} & [\mathbf{K}_{rl}^2] & [\mathbf{K}_{rr}^2 - \mathbf{K}_{ll}^3 + \mathbf{D}_{rl}^2] & -[\mathbf{K}_{lr}^3] & \mathbf{0} \\ \mathbf{0} & \mathbf{0} & [\mathbf{K}_{rl}^3] & [\mathbf{K}_{rr}^3 - \mathbf{K}_{ll}^4 + \mathbf{D}_{rl}^3] & -[\mathbf{K}_{lr}^4] \\ \mathbf{0} & \mathbf{0} & \mathbf{0} & [\mathbf{K}_{rl}^4] & [\mathbf{K}_{rr}^4 + \mathbf{B}_{rl}^2] \end{bmatrix}^{-1}. \tag{59}$$

In equation (58) the control forces applied to two bearings are designated by $\hat{\mathbf{Q}}_1$ and $\hat{\mathbf{Q}}_2$, while the vertical displacements measured are elements of the vectors $\bar{\mathbf{q}}_1$, $\bar{\mathbf{q}}_2$ and $\bar{\mathbf{q}}_3$. When there is no external forces on the lumped discs,

$$\bar{\mathbf{Q}}_1 = \bar{\mathbf{Q}}_2 = \bar{\mathbf{Q}}_3 = \mathbf{0}. \tag{60}$$

Considering equation (60) the multivariable frequency response matrix of the system can be computed from elements of the flexibility matrix in equation (59) by using equation (43):

$$G_{11}(\mathrm{j}\omega) = \Lambda_{5,2}(\mathrm{j}\omega),\ G_{22}(\mathrm{j}\omega) = \Lambda_{13,18}(\mathrm{j}\omega),\ G_{31}(\mathrm{j}\omega) = \Lambda_{9,2}(\mathrm{j}\omega), \tag{61}$$

$$G_{21}(\mathrm{j}\omega) = \Lambda_{13,2}(\mathrm{j}\omega),\ G_{12}(\mathrm{j}\omega) = \Lambda_{5,18}(\mathrm{j}\omega),\ G_{32}(\mathrm{j}\omega) = \Lambda_{9,18}(\mathrm{j}\omega). \tag{62}$$

Using the elements of the multivariable frequency response matrix displayed in equations (61) and (62) and the algorithm for the estimation of the second order transfer functions, which is described by equations (44)–(57) the transfer function matrix of the rotor-bearing system can be computed.

With a configuration where only one sensor is located at the middle disc and the actuators are placed at bearings 1 and 2 the system has two input and one output, hence

$$Y_3(s) = [G'_{31}(s)\ \ G'_{32}(s)]\begin{bmatrix} Q_1(s) \\ Q_2(s) \end{bmatrix}, \tag{63}$$

where the transfer functions in equation (63) are

$$G'_{31}(s) = \frac{1}{(0{\cdot}000556s^2 + 0{\cdot}0030s + 7{\cdot}002)}, \tag{64}$$

$$G'_{32}(s) = \frac{1}{(0{\cdot}000549s^2 + 0{\cdot}0030s + 6{\cdot}864)}. \tag{65}$$

Figures 6(a) and 6(b) show how close the estimated transfer functions (64) and (65) are to the actual transfer function in equations (61) and (62). These figures also show that at the point $\omega = 112$ rad/s there is a peak in the frequency response curves. This confirms the validity of the result obtained for the whirl frequency of the rotor.

In the configuration where two sensors are located at discs 1 and 2, while actuators are placed at bearings 1 and 2 the system then has two inputs and two outputs, hence

$$\begin{bmatrix} Y_1(s) \\ Y_2(s) \end{bmatrix} = \begin{bmatrix} G'_{11}(s) & G'_{12}(s) \\ G'_{21}(s) & G'_{22}(s) \end{bmatrix}\begin{bmatrix} Q_1(s) \\ Q_2(s) \end{bmatrix}, \tag{66}$$

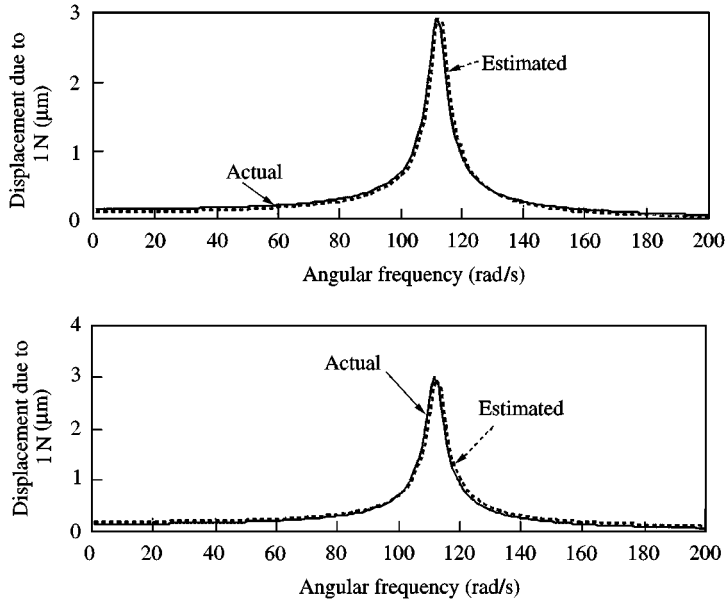

Figure 6. (a) Frequency response indicate actual G31, estimated G31. (b) Frequency response, indicate actual G32, estimated G32.

where the transfer functions in (66) are

$$G'_{11}(s) = \frac{1}{(0{\cdot}000758s^2 + 0{\cdot}0041s + 9{\cdot}537)}, \tag{67}$$

$$G'_{21}(s) = \frac{1}{(0{\cdot}000815s^2 + 0{\cdot}0041s + 10{\cdot}255)}, \tag{68}$$

$$G'_{22}(s) = \frac{1}{(0{\cdot}000794s^2 + 0{\cdot}0043s + 9{\cdot}989)}, \tag{69}$$

$$G'_{12}(s) = \frac{1}{(0{\cdot}000737s^2 + 0{\cdot}0040s + 9{\cdot}273)}, \tag{70}$$

Figures 7(a) and 7(b) and also Figures 8(a) and 8(b) show that the estimated transfer functions (67)–(70) are very close to the actual transfer functions in equations (61) and (62). These figures also show that when $\omega = 112$ rad/s there is a peak in the frequency response curves.

When three sensors located at discs 1, 2 and 3 and the actuators are placed at bearings 1 and 2 the system has two inputs and three outputs, hence

$$\begin{bmatrix} Y_1(s) \\ Y_2(s) \\ Y_3(s) \end{bmatrix} = \begin{bmatrix} G'_{11}(S) & G'_{12}(s) \\ G'_{21}(s) & G'_{22}(s) \\ G'_{31}(s) & G'_{32}(s) \end{bmatrix} \begin{bmatrix} Q_1(s) \\ Q_2(s) \end{bmatrix}. \tag{71}$$

The second order transfer functions in equation (71) are given by equations (64), (65) and also (67)–(70).

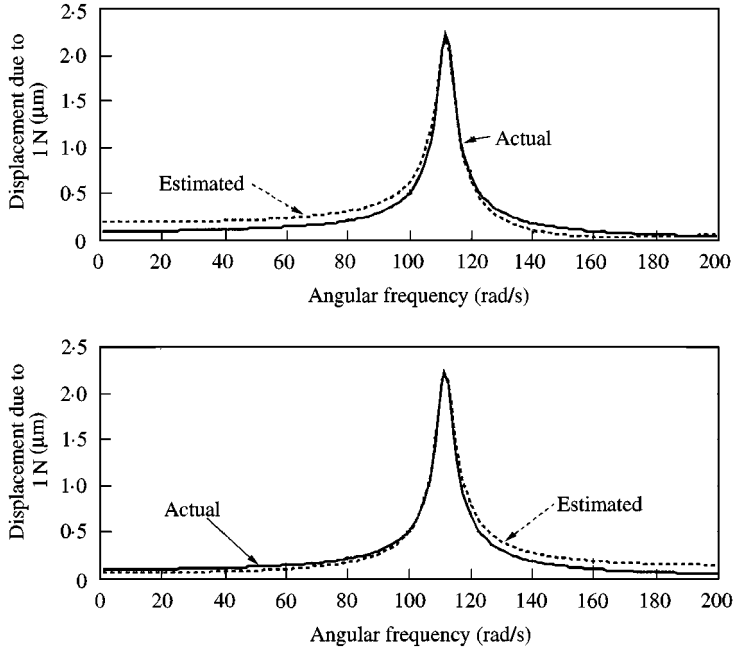

Figure 7. (a) Frequency response indicate actual G11, estimated G11. (b) Frequency response, indicate actual G12, estimated G12.

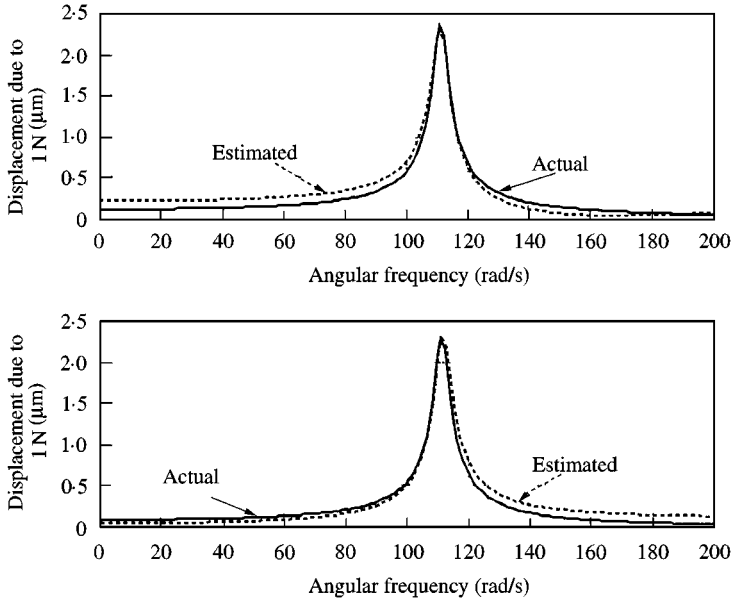

Figure 8. (a) Frequency response indicate actual G22, estimated G22. (b) Frequency response, indicate actual G21, estimated G21.

CONCLUSION

Lumped modelling procedures are generally employed in the analysis of "active vibration control" of rotor-bearing systems [3]. This results in high order system models, which in turn create difficulties in design of controllers [2]. An experimental study based on these theories suggests that an efficient way for controlling the vibrational amplitude is by implementing a single magnetic actuator with a position which is determined by an on-line computer [24]. However, a more practical scheme can be achieved by putting the magnetic actuators at the supporting bearings with the measured vibration amplitude of the rotors as outputs [25]. In this paper, a method is proposed for the computation of multi-input, multi-output, transfer function matrix description of rotor-bearings system. This results in greater accuracy and lower order representation enabling, multivariable frequency domain techniques to be implemented for controller design purposes.

REFERENCES

1. H. D. NELSON and J. M. MCVAUGH 1976 *Transactions of the ASME, Journal of Engineering for Industry* **98**, 593–600. The dynamics of rotor bearing systems using finite elements.
2. G. W. FAN, H. D. NELSON and M. P. MIGNOLET 1993 *Transactions of the ASME Journal of Engineering for Gas Turbines and Power* **115**, 307–330. Optimal output feedback control of asymmetric systems using complex modes.
3. C. R. BURROWS and M. N. SAHINKAYA 1983 *Proceedings of Royal Society of London, Part A* **386**, 77–94. Vibration control of multi-mode rotor-bearing systems.
4. N. O. MYKLESTAD 1944 *Journal of Aerosol Science*, Vol. 11, 153–162. A new method of calculating natural modes of uncoupled bending vibration of aeroplane wings and other type of beams.
5. M. A. PROHL 1945 *Journal of Applied Mechanics* **12**, 142–148. A general method for calculating critical speeds of flexible rotors.

6. J. W. LUND 1974 *Transactions of the ASME, Journal of Engineering for Industry*, Vol. 96, 509–517. Stability and damped critical speeds of a flexible rotor in fluid-film bearings.
7. R. FIROOZIAN and H. ZHU 1991 *Proceedings of the Institution of Mechanical Engineers Part C* **205**, 131–137. A hybrid method for the vibration analysis of rotor-bearing systems.
8. A. C. LEE, Y. KANG and S. L. LIU 1991 *ASME Journal of Applied Mechanics* **58**, 776–783. A modified transfer matrix method for linear rotor-bearing systems.
9. R. K. LIVESLEY 1964 *Matrix Methods of Structural Analysis*. Oxford: Pergamon Press.
10. F. W. WILLIAMS and W. H. WITTRICK 1970 *International Journal of Mechanical Sciences* **12**, 781–791. An automatic computational procedure for calculating natural frequencies of skeletal structures.
11. P. H. KULLA 1997 *Finite Element in analysis and Design* **26**, 97–114. High precision finite elements.
12. G. CURTI, F. A. RAFFA and F. VATTA 1991 *Tribology Transactions* **34**, 81–85. The dynamic stiffness matrix method in the analysis of rotating systems.
13. F. A. RAFFA and F. VATTA 1996 *Transactions of the ASME, Journal of Vibration and Acoustics* **118**, 333–339. The dynamic stiffness method for linear rotor–bearing systems.
14. R. WHALLEY 1988 *Proceedings of the Institution of Mechanical Engineers Part C* **202**, 421–429. The response of distributed-lumped parameter systems.
15. M. ALEYAASIN, R. WHALLEY and M. EBRAHIMI 2000 *Computer Methods in Applied Mechanics and Engineering*. Vibration analysis of distributed-lumped rotor systems (in press).
16. H. OKAMURA, A. SHINNO, T. YAMANAKA, A. SUZUKI and K. SOGABE 1995 *Transactions of the ASME, Journal of Vibration and Acoustics* **117**, 70–79. Simple modelling and analysis for crankshaft three dimensional vibrations, Part 1: background and application to free vibrations.
17. H. OKAMURA and A. SHINNO 1988 *Multibody Dynamic Conference: C23/88, IMechE*, 95–108. Dynamic stiffness matrix method for the three dimensional analysis of crankshaft vibrations.
18. C. W. CHEN, J. N. JUANG and G. LEE 1994 *Transactions of the ASME, Journal of Vibration and Acoustics* **116**, 523–528. Frequency domain state-space system identification.
19. Cambridge Control Ltd 1998 *Multivariable Frequency Domain Toolbox For Use with MATLAB*.
20. M. ALEYAASIN 1998 *Internal Report, CSDG135, Department of Mechanical Engineering University of Bradford*. The response of distributed-lumped systems using inverse fourier transforms.
21. C. F. BEARDS 1995 *Engineering Vibration Analysis with Application to Control Systems*. London: Edwards Arnold.
22. The Math Works Inc. MA 1997 *Using MATLAB Version 5*.
23. B. D. BUNDAY 1984 *Basic Optimization Methods*. London: Edward Arnold.
24. C. R. BURROWS, M. N. SAHINKAYA and C. CLEMENTS 1989 *Proceedings of Royal Society London, Part A* **422**, 123–146. Active vibration control of flexible rotors: an experimental and theoretical study.
25. H. HABERMANN and G. LIARD 1980 *Tribology International* **13**, 85–89. An active magnetic bearings system.

APPENDIX A

For the computation of the stiffness and damping coefficients of a journal bearing the following data is required. (1) length of the journal bearing l, (2) radius of the journal, R, (3) radial clearance c, (4) lubricant viscosity μ, and (5) angular velocity of the journal ω.

Then the load-carrying capacity of the bearing would be

$$P = \sqrt{F_r^2 + F_s^2}, \tag{A1}$$

where

$$F_r = -\frac{\omega\varepsilon^2\mu l^3 R}{c^2(1-\varepsilon^2)},$$
$$F_s = \frac{\omega\pi\varepsilon\mu l^3 R}{4c^2(1-\varepsilon^2)^{1.5}}. \tag{A2}$$

The variable ε in equation (A2) is the eccentricity ratio.

The following successive steps are necessary:

Step 1. Using l, R, c, μ, and ω compute the parameters

$$K_r = \frac{\omega\mu I^3 R}{c^2}, \qquad K_s = \frac{\omega\pi\mu I^3 R}{4c^2}. \tag{A3}$$

Step 2. When the load carried by bearing P is known the eccentricity ratio ε can be determined by finding the roots of this fourth order equation:

$$P^2\varepsilon^4 + (K_s^2 - 4P^2)\varepsilon^3 + (6P^2 - K_r^2 - K_s^2)\varepsilon^2 - 4P^2\varepsilon + P^2 = 0. \tag{A4}$$

Step 3. Compute the following dimensionless parameters:

$$k_{rr} = \frac{8(1+\varepsilon^2)}{(1-\varepsilon^2)[\pi^2(1-\varepsilon^2)+16\varepsilon^2]^{0\cdot5}}, \qquad k_{rs} = \frac{\pi(1-\varepsilon^2)^{0\cdot5}}{\varepsilon[\pi^2(1-\varepsilon^2)+16\varepsilon^2]^{0\cdot5}}, \tag{A5}$$

$$k_{sr} = \frac{\pi(1+2\varepsilon^2)}{\varepsilon(1-\varepsilon^2)^{0\cdot5}[\pi^2(1-\varepsilon^2)+16\varepsilon^2]^{0\cdot5}}, \qquad k_{ss} = \frac{4}{[\pi^2(1-\varepsilon^2)+16\varepsilon^2]^{0\cdot5}}. \tag{A6}$$

Step 4. Compute the angle ψ and the parameters

$$\tan\psi = \frac{|F_s|}{|F_r|} = \frac{\pi(1-\varepsilon^2)^{0.5}}{4\varepsilon}, \tag{A7}$$

$$c_{rr} = c_{sr} = 2k_{ss}, \quad c_{ss} = 2k_{rs}, \quad c_{rr} = 2k_{sr}. \tag{A8}$$

Step 5. Compute the stiffness of the bearing from the equation

$$\begin{bmatrix} K_{yy} \\ K_{yz} \\ K_{zy} \\ K_{zz} \end{bmatrix} = \frac{P}{c} \begin{bmatrix} k_{rr} & k_{ss} & (k_{sr}-k_{rs}) \\ k_{rs} & k_{sr} & (k_{rr}-k_{ss}) \\ k_{sr} & k_{rs} & (k_{ss}-k_{rr}) \\ k_{ss} & k_{rr} & (k_{rs}-k_{sr}) \end{bmatrix} \begin{bmatrix} \cos^2\psi \\ \sin^2\psi \\ \cos\psi\sin\psi \end{bmatrix}, \tag{A9}$$

and damping coefficients of the bearing from

$$\begin{bmatrix} C_{yy} \\ C_{yz} \\ C_{zy} \\ C_{zz} \end{bmatrix} = \frac{P}{c\omega} \begin{bmatrix} c_{rr} & c_{ss} & (c_{rs}+c_{sr}) \\ -c_{rs} & c_{sr} & (c_{rr}-c_{ss}) \\ -c_{sr} & c_{rs} & (c_{rr}-c_{ss}) \\ c_{ss} & c_{rr} & -(c_{rs}+c_{sr}) \end{bmatrix} \begin{bmatrix} \cos^2\psi \\ \sin^2\psi \\ \cos\psi\sin\psi \end{bmatrix}. \tag{A10}$$

APPENDIX B: NOMENCLATURE

A	area of the shaft cross-section
E	shaft modulus
$G_{ij}(j\omega)$	elements of the system frequency response matrix
$G'_{ij}(s)$	elements of the estimated system transfer function
I	second moment of area in bending
J_p, J_t	polar and transverse moment of inertia of disk
L	length of each distributed part

M_y	bending moment function, y direction
M_z	bending moment function, z direction
Q_y	shear force function, y direction
Q_z	shear force function, z direction
$[\bar{\mathbf{Q}}_i]$	force vector at the ith element
$[\bar{\mathbf{q}}_i]$	displacement vector at the ith element
R	characteristic determinant of the system
s	Laplace transform matrix
$\mathbf{T}$	overall tansfer matrix
Y	vertical displacement function
Z	horizontal displacement function
θ	slope function in vertical plane
ρ	density of distributed shaft
ϕ	slope function in horizontal plane
Γ	auxiliary Laplace variable
$\mathbf{\Phi}_l$	transfer matrix of the lumped disc element
$\mathbf{\Phi}_b$	transfer matrix of the lumped bearing element
$\mathbf{\Phi}_d$	transfer matrix of the distributed shaft element
Ω	rotational speed of the shaft
$\mathbf{\Lambda}$	dynamic stiffness matrix of rotor system